Space Sci Rev (2009) 148: 225–232
DOI 10.1007/s11214-009-9566-x

Atom-Based Test of the Equivalence Principle

Sebastian Fray · Martin Weitz

Received: 3 April 2009 / Accepted: 7 July 2009 / Published online: 25 July 2009

Abstract We describe a test of the equivalence principle with quantum probe particles based on atom interferometry. For the measurement, a light pulse atom interferometer based on the diffraction of atoms from effective absorption gratings of light has been developed. A differential measurement of the Earth's gravitational acceleration g for the two rubidium isotopes ^{85}Rb and ^{87}Rb has been performed, yielding a difference $\Delta g/g = (1.2 \pm 1.7) \times 10^{-7}$. In addition, the dependence of the free fall on the relative orientation of the electron to the nuclear spin was studied by using atoms in two different hyperfine states. The determined difference in the gravitational acceleration is $\Delta g/g = (0.4 \pm 1.2) \times 10^{-7}$. Within their experimental accuracy, both measurements are consistent with a free atomic fall that is independent from internal composition and spin orientation.

Keywords Quantum mechanics · Gravity · Equivalence principle · Atom interferometer

A unification of gravitational and quantum theory is a still unsolved problem in today's physics. Much of the current research efforts in theoretical approaches like the string theory are motivated by this quest (Schutz and Damour 2009). To verify corresponding theoretical models, critical experiments have to be performed which combine both domains, quantum mechanics and gravity. One class of experiments, which give a deep foundation to gravity, represents tests of Einstein's equivalence principle. This fundamental principle states that all bodies, regardless of their internal composition, are affected by gravity in a universal way, i.e. they in the absence of other forces fall with the same acceleration. For macroscopic objects, tests of the equivalence principle have been performed since the early days of modern

S. Fray (✉)
Max-Planck-Institut für Quantenoptik, Hans-Kopfermann-Str. 1, 85748 Garching, Germany
e-mail: sebf@gmx.net

M. Weitz
Institut für Angewandte Physik, Wegeler Str. 8, 53115 Bonn, Germany

Present address:
S. Fray
Qimonda AG, Am Campeon 1-12, 85579 Neubiberg, Germany

physics (Su et al. 1994). Atomic based approaches to the equivalence principle have been proposed (Audretsch et al. 1993; Viola and Onofrio 1997), motivated by the challenge to provide new tests of theories which merge quantum mechanics and relativity.

Before proceeding, let us point out that the first atom based tests of general relativity are the Pound-Rebka experiments that investigate the gravitational redshift. At present, the achieved relative accuracy of this small shift between atomic clocks in different reference frames is 7×10^{-5} (Vessot et al. 1980). For a comparison between different tests of the equivalence principle, see (Nordtvedt 2002). We also remark that questions whether a spin-mass coupling exists have been considered theoretically (Lämmerzahl 1998). A measurement on spin-mass interaction was performed by comparing the weight of oppositely spin polarized bulk matter (Hsieh et al. 1989).

In recent years matter-wave interferometric techniques have proven to allow for measurements of inertial effects (Berman 1997). In particular, atom interferometers were used to carry out precision measurements of the rotation (Gustavson et al. 1997, 2000) and the Earth's gravitational acceleration (Peters et al. 1999, 2001).

Here we describe an experiment testing the equivalence principle on an atomic basis. The experiment represents a proof of principle demonstration extending the free fall equivalence principle test to atoms as quantum probe particles, see Fray et al. (2004) for an earlier, detailed account of our measurement. With an atom interferometer, the Earth's gravitational acceleration of the two different isotopes ^{85}Rb and ^{87}Rb of the rubidium atom was compared to a relative accuracy of 1.7×10^{-7}. We also studied the free fall acceleration as a function of relative orientation of nuclear to electron spin to an accuracy of 1.2×10^{-7} by comparing interference patterns measured with ^{85}Rb atoms prepared in two different hyperfine ground states. Within the experimental accuracies, the obtained results of this 2004 measurement are consistent with no violation of the equivalence principle. We expect that technical improvements will in the future allow for extremely critical test of the equivalence principle using atoms as probe particles.

For the measurement, a light pulse atom interferometer based on the diffraction of atoms from standing light waves acting as effective absorption grating has been developed. In each of the matter wave beam splitters, the atomic de Broglie wave is diffracted into a coherent superposition of eigenstates, which differ only in momentum and not in their internal atomic states. We note that this is in contrast to several earlier experiments investigating inertial effects with atom interferometry, where the interfering paths were in different internal atomic states so that the difference in ac-Stark shift can contribute to the systematic error budget (Berman 1997). In our experiment (Fray et al. 2004) the different paths are in the same internal state, so that this source of systematic uncertainties is reduced. We note that several recently developed atom interferometers with large spatial separation between paths and correspondingly high sensitivity also use same internal states of interferometer paths (Müller et al. 2009; Cladé et al. 2009).

We use three standing wave light pulses as atomic beam splitters, which are applied to an ensemble of cold rubidium atoms launched on a vertical ballistic trajectory in an atomic fountain setup. The scheme of the atom interferometer is shown in Fig. 1. The frequency of the atomic beam splitter light is tuned resonantly to an open transition from a ground state $|g_D\rangle$ to a spontaneously decaying excited state $|e\rangle$. The spatially dependent intensity distribution of the standing light wave will then lead to a pumping of the atom that pass through the intensity antinodes into magnetic and hyperfine sublevels that are not any more detected. On the other hand, atoms close to the nodes will remain in the ground state $|g_D\rangle$. After the pulses, only the population in this state is detected. Hence the standing light wave forms an effective absorption grating, where due to the spatial periodicity of $\lambda/2$ an incident atomic

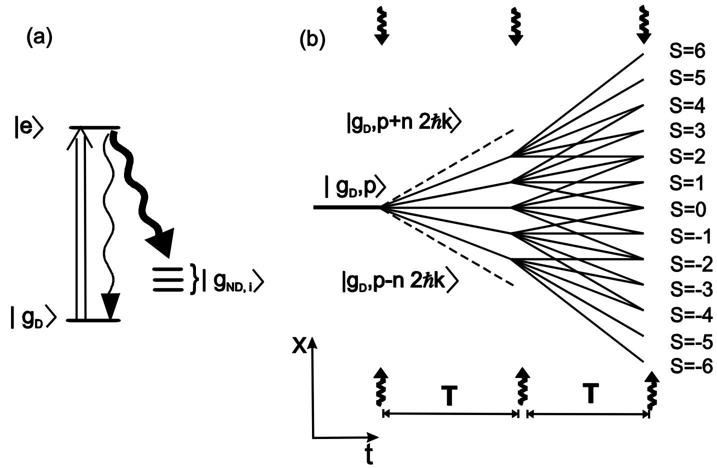

Fig. 1 (**a**) Simplified level scheme, where $|g_D\rangle$ denotes the ground state detected at the interferometer output, $|g_{ND,i}\rangle$ (ground) states that are not detected, and $|e\rangle$ the electronically excited state. (**b**) Outline of an atomic interferometer realized with three effective absorption gratings of light. The different families of interfering wave packets are numbered by the index s

wave function with the initial momentum p is split into a series of eigenstates differing in momentum by an integer multiple of $2\hbar k$. The number of paths increases with higher pulse area, however the transmission efficiency decreases.

In the beginning of the atomic free fall at time $t = 0$ the first optical pulse in our interferometric scheme splits an atomic wave packet into several distinct paths. Later on at a time $t = T$ a second pulse is applied, which again leads to a diffraction and coherently splits up the paths. At the end of the atomic free fall at time $t = 2T$, several paths spatially overlap in a series of families of wave packets and we expect that the wave nature leads to a spatial atomic interference structure. To read out this periodic fringe pattern, we again apply a resonant optical pulse tuned to the open transition and thus overlay the light's intensity distribution with the atomic density. The periodic pattern can now be read out by scanning the position of this third grating and monitoring the number of transmitted atoms in the ground state. For technical reasons, we actually leave the position of the optical grating constant and instead vary the pulse spacing T, which due to Earth's gravitational acceleration changes the position of the atomic interference pattern relative to the standing light wave and this way allows for an observation of the fringe pattern.

The expected fringe pattern is calculated in detail elsewhere (Fray et al. 2004). Here we only show the results of the calculation. Considering the spatial density of atoms in the ground state $\rho_D(x) = \int dp\, g(p)\langle x|\psi\rangle\langle\psi|x\rangle$ the following expression can be derived for $\rho(x)$ at the position of the third interferometer pulse:

$$\rho(x) = \sum_{s=-\infty}^{\infty} ||\Psi_s(x)\rangle|^2$$

with

$$|\Psi_s\rangle = \sum_{n=-\infty}^{\infty} I_n\left(\frac{\Omega^2}{\Gamma}\tau_1\right) I_{s-2n}\left(\frac{\Omega^2}{\Gamma}\tau_2\right) \times \exp\left\{-(\Omega^2/\Gamma)(\tau_1+\tau_2)\right\} \exp\left\{i(sn-n^2)2\omega_r T\right\} \exp\{-in2kx\},$$

Fig. 2 Schematic view of the atomic fountain setup. About 10^9 rubidium atoms are captured in a magneto-optical trap, cooled to a temperature of 6 μK and launched onto a vertical ballistic trajectory by laser forces. A temporal sequence of three resonant optical standing wave pulses is used as beam splitters for the atomic matter waves, realizing an atom interferometer for the two rubidium isotopes respectively

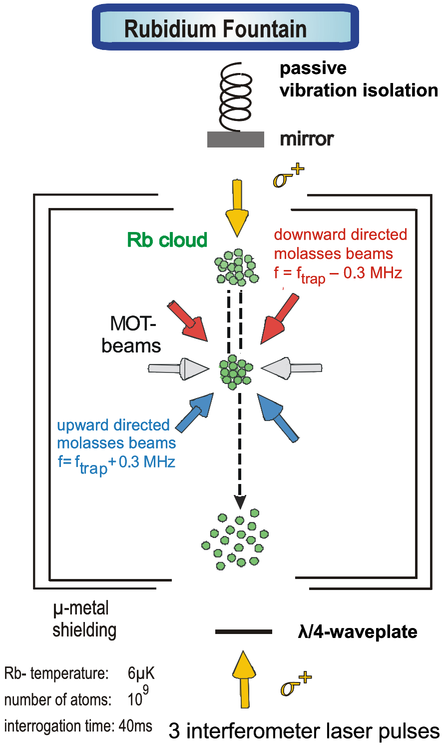

where Ω denotes the Rabi frequency, Γ the spontaneous decay rate of the exited state, $I_n(x)$ the modified Bessel function and $\tau_{1,2}$ the pulse length of the first and second pulse respectively. Further, $\omega_r = 2\hbar k^2/m$ denotes the recoil energy of a two photon transition in frequency units. Introducing the Earth's gravitational acceleration in the above calculation, the exponential factor has to be extended by a phase term $(-inkgT^2)$. While the expected density modulation is near sinusoidal in the unsaturated case [i.e. $(\Omega^2/\Gamma)\tau \leq 1$], the fringe pattern sharpens to an Airy-function-like multiple-beam pattern for larger pulse energies (Weitz et al. 1996; Hinderthür et al. 1997).

Our experimental apparatus is illustrated in Fig. 2. It is based on an ultrahigh vacuum chamber in which a magneto-optic trap captures one billion cold rubidium atoms from the thermal rubidium metal vapor. The atoms are then launched onto a vertical upwards moving ballistic trajectory by acoustooptically shifting the molasses beams' frequencies to a moving molasses traveling upwards. The temperature of the atomic ensemble at the beginning of the launch is 6 μK. On their ballistic flight the atoms reach the upper turning point and fall down. During the parabolic flight of the atoms the three optical beam splitting pulses are applied to realize the atom interferometer. To prepare the atomic ensemble in a magnetic field insensitive ground state sublevel a suitable sequence of microwave pulses and resonant optical pulses is applied. This state selection procedure needs to be repeated also after the atomic beam splitting sequence for state analysis. The remaining atomic population is detected by a FM-fluorescence spectroscopic technique, to allow for a distinction of the cold atoms from the Doppler-broadened background rubidium vapor.

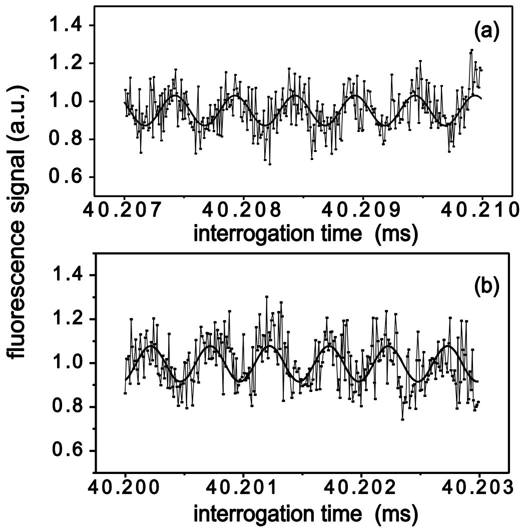

Fig. 3 Typical atomic interference signals as a function of pulse spacing T varied in narrow regions near $T = 40$ ms. The signals were recorded (**a**) for ^{85}Rb atoms with the optical field tuned to the $F = 2 \rightarrow F' = 3$ component and (**b**) for ^{87}Rb atoms using the $F = 1 \rightarrow F' = 2$ component of the rubidium D1-line respectively. The visible phase shift between the two interference patterns is caused by a slightly different transition frequency for the two isotopes

The atomic beam splitter light is generated by an injection locked master-slave diode laser system that is locked to the rubidium D1-line near 795 nm. The emitted radiation passes a series of two acoustooptical modulators used for switching, a single mode optical fiber and is then expanded to a 3 cm Gaussian beam diameter and directed into the vacuum chamber. After passing the chamber, the beam is retroreflected with a mirror. The generated pulsed optical standing wave has a duration of 200 ns and an intensity of 3 mW/cm^2 per direction at the position of the atomic cloud, which is sufficient for an effective pumping of atoms near the antinodes of the standing light wave. Since the retroreflecting mirror defines the position of the standing light wave, it is crucial to suppress vibrational coupling onto this mirror. For this reason we use a floating table for the setup and a retroreflecting mirror that is passively isolated from external vibrations. The mirror is suspended on a 2.5 m long ribbon string fixed at the ceiling. Frictionless motion was provided by mounting the mirror on an air bearing.

Measured interference patterns are shown in Fig. 3a and 3b as a function of the spacing T between the beam splitting pulses obtained using ^{85}Rb and ^{87}Rb atoms respectively. The data points shown in both plots can be well fitted sinusoidal functions (solid line). We attributed the sinusoidal form of the fringe pattern to the issue that the main contribution to the signal is due to two-path interference. From the fit, the relative phase of the fringe pattern can be determined with an accuracy of 0.02 of a period. The observed fringe contrast is 20 per cent for small interrogation times T and reduces to some 9 per cent for the shown fringe patterns with high gravitational sensitivity recorded near $T = 40$ ms. This loss of fringe contrast for longer coherence times is attributed to residual mechanical vibrations of the interferometer beams retroreflecting mirror. On the other hand, even at small interrogation times the fringe contrast is below the theoretical value of 90%. We attribute this mainly to residual reflection of the vacuum windows, which cause an intensity imbalance between the forward and the backward propagation wave of approximately 2%. The residual reflection is mainly caused by the deposition of rubidium vapor on the vacuum windows of our apparatus.

To determine the total gravitational phase experienced by the atoms at an interrogation time of 40 ms, we record fringe patterns also at the smaller interrogation times of 2, 6,

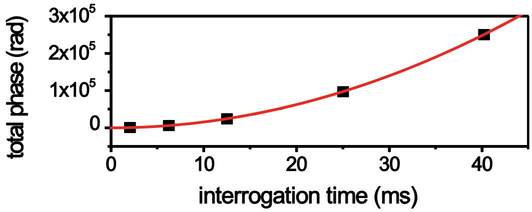

Fig. 4 Total atom phase between adjacent paths for the ^{85}Rb interferometer as a function of the interrogation time T between the beam splitting pulses. The shown solid line is a parabolic fit

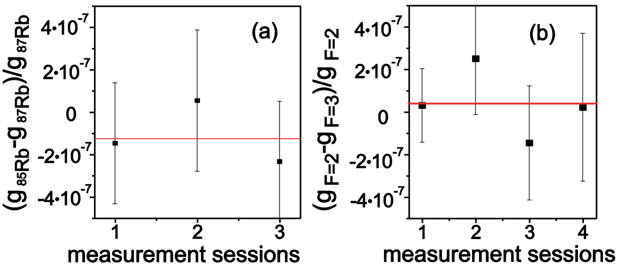

Fig. 5 Measured difference of the gravitational acceleration in individual measurement sessions (*dots*) and total average (*vertical line*) for (**a**) the two different isotopes ^{85}Rb and ^{87}Rb and (**b**) for atoms (^{85}Rb) in the different hyperfine ground states $F = 2$ and $F = 3$

12, 18 ms respectively and monitor the accumulation of the gravitational phase. In this way, phase ambiguities due to the periodic character of the fringe pattern can be avoided. Figure 4 shows typical recorded data (dots) along with a fit to the expected parabolic curve (solid), while the gravitational acceleration g was left as a free parameter. The precision of gravitational acceleration measurement is determined by ratio of the phase accuracy and the total phase $\Delta g/g = \Delta\phi/\phi$. At 40 ms the interference pattern starts at roughly the 40000th fringe, and accounting for the determination of the fringe position in a single scan this results in a typical relative accuracy of the total phase: $\Delta g/g = \Delta\phi/\phi \cong 0.02/40000 = 5 \times 10^{-7}$. By recording multiple of such fringe patterns, the earth's gravitational acceleration can in 6 hours of data acquisition be determined to a statistical accuracy of 8×10^{-8}. We expect that considerable longer interrogation times and thus considerable further increased sensitivities should be possible with active vibration isolation techniques (Hensley et al. 1999).

In our measurement we have compared the Earth's gravitational acceleration of ^{85}Rb atoms in the $F = 2$, $m_F = 0$ hyperfine ground state with that experienced by ^{87}Rb atoms in $F = 1$, $m_F = 0$. The data has been recorded in three measurement sessions, each corresponding to the data recorded during one day. In every session fringe patterns at interrogation times $T \approx 40$ ms were recorded for both of the isotopes. A switching between atomic species could be performed very easily by locking the frequency of the cooling and atomic interferometer lasers respectively to the appropriate atomic transition. We typically alternated between measurements investigating the isotopes ^{85}Rb and ^{87}Rb respectively in temporal periods of 40 minutes each. As the switching rate between isotopes is faster than the tidal period, and due to the averaging effect we do not expect tidal changes of the Earth's gravitational acceleration (a few 10^{-7} in one day, Peters et al. 1999, 2001) to affect the accuracy of our differential measurement at the present level of precision. In future, we expect that atoms based tests of the equivalence principle will at some level of precision require independent laser systems for each of the isotopes, so that the measurements for the two isotopes can be performed (quasi-)simultaneously.

Figure 5a shows the results for the relative difference of the Earth's gravitational acceleration measured in the three sessions along with a horizontal line that represents the total average. This final value for the difference of the gravitational acceleration is $(g_{85\text{Rb}} - g_{87\text{Rb}})/g_{85\text{Rb}} = (1.2 \pm 1.7) \times 10^{-7}$. The quoted error here corresponds to the estimated total uncertainty. In this differential measurement, systematic errors due to misalignment of the beams, wave front curvature, and Coriolis forces largely cancel, and at the present level of accuracy clearly can be neglected. Moreover, as all paths of our atom interferometer are in the same internal state, systematic effects due to the second order Zeeman shift occur only in the presence of a magnetic field gradient. The estimated systematic uncertainty due to field inhomogeneities (8 mG/cm) is for our present apparatus estimated to be 5×10^{-11}, which is also clearly negligible. Within the quoted uncertainties, our above given value agrees well with the expected result of an identical gravitational acceleration of the two rubidium isotopes in the Earth's field.

In the measurements, the gravitational acceleration experienced by atoms in two different hyperfine ground states has been compared. For this measurement, interference fringes were recorded using ^{85}Rb atoms prepared selectively in the atomic hyperfine ground states $F = 2$, $m_F = 0$ and $F = 3$, $m_F = 0$ respectively. Results for the difference in the measured Earth's gravitational acceleration for atoms prepared in the corresponding hyperfine ground states are shown in Fig. 5b. The obtained average value is $(g_{F=3} - g_{F=2})/g_{F=2} = (0.4 \pm 1.2) \times 10^{-7}$. Within the quoted experimental uncertainty, no difference in the Earth's gravitational acceleration for atoms in two different hyperfine ground states is observed.

In conclusion, an atom interferometer based on pulsed effective absorption gratings of light has been developed. The atom interferometer has been used to carry out the to our knowledge first atom based test of the equivalence principle.

In the future, technical improvements like an active vibration isolation allowing for longer interrogation times and improvements in wave front quality that can yield multiple beam interference signals with sharp principle maxima, where in contrast to earlier schemes the path number is not limited by the internal structure (Weitz et al. 1996; Hinderthür et al. 1997). Further, the use of dilute Bose-Einstein condensed samples can due to their small velocity spread of atoms increase the obtainable accuracy. We expect that atom interferometers can allow for extremely critical tests of the equivalence principle based on quantum probe particles. Experimental efforts along this goal are described by the contribution of M. Kasevich in this volume. Ultimately space based atom interferometers are expected to yield a still further increased precision (Ertmer et al. 2009).

References

J. Audretsch, U. Bleyer, C. Lämmerzahl, Phys. Rev. A **47**, 4632 (1993)
See, e.g., P. Berman, *Atom Interferometry* (Academic Press, San Diego, 1997).
P. Cladé, S. Guellati-Khélifa, F. Nez, F. Biraben, Phys. Rev. Lett. **102**, 240402 (2009)
See, e.g.: W. Ertmer et al., Exp. Astron. **23**, 611 (2009)
S. Fray, C. Alvarez Dies, T.W. Hänsch, M. Weitz, Phys. Rev. Lett. **93**, 240404 (2004)
T.L. Gustavson, P. Bouyer, M.A. Kasevich, Phys. Rev. Lett. **78**, 2046 (1997)
T.L. Gustavson, A. Landragin, M.A. Kasevich, Class. Quantum Gravity **17**, 2385 (2000)
J.M. Hensley et al., J. Sci. Instrum. **70**, 2735 (1999)
H. Hinderthür et al., Phys. Rev. A **56**, 2085 (1997)
C.H. Hsieh et al., Mod. Phys. Lett. A **4**, 1597 (1989)
C. Lämmerzahl, in *Proceedings of the International School of Cosmology and Gravitation, Course XV*, ed. by P.G. Bergmann et al. (World Scientific, Singapore, 1998) and references therein

H. Müller, S. Chiow, S. Herrmann, S. Chu, Phys. Rev. Lett. **102**, 240403 (2009)
K. Nordtvedt, gr-qc/0212044 (2002)
A. Peters, C. Keng Yeow, S. Chu, Nature (London) **400**, 849 (1999)
A. Peters, K.Y. Chung, S. Chu, Meterologia **38**, 25 (2001)
See, e.g. the contributions by B. Schutz T. Damour, Space Sci. Rev. (2009, this issue)
Y. Su et al., Phys. Rev. D **50**, 3614 (1994) and references therein
R.F.C. Vessot et al., Phys. Rev. Lett. **45**, 2081 (1980)
L. Viola, R. Onofrio, Phys. Rev. D **55**, 455 (1997)
M. Weitz, T. Heupel, T.W. Hänsch, Phys. Rev. Lett. **77**, 2356 (1996)